



Simulation of diffractive and non-diffractive processes at the LHC energy with the PYTHIA and PHOJET MC event generators

J.P. Guillaud, A.E. Sobol

► **To cite this version:**

J.P. Guillaud, A.E. Sobol. Simulation of diffractive and non-diffractive processes at the LHC energy with the PYTHIA and PHOJET MC event generators. 2004, pp.1-20. in2p3-00021835

HAL Id: in2p3-00021835

<http://hal.in2p3.fr/in2p3-00021835>

Submitted on 10 Sep 2004

HAL is a multi-disciplinary open access archive for the deposit and dissemination of scientific research documents, whether they are published or not. The documents may come from teaching and research institutions in France or abroad, or from public or private research centers.

L'archive ouverte pluridisciplinaire **HAL**, est destinée au dépôt et à la diffusion de documents scientifiques de niveau recherche, publiés ou non, émanant des établissements d'enseignement et de recherche français ou étrangers, des laboratoires publics ou privés.

LAPP-EXP 2004-06

July 2004

**Simulation of diffractive and non-diffractive processes
at the LHC energy with the PYTHIA and PHOJET
MC event generators.**

J.P. Guillaud, A.Sobol

LAPP, IN2P3-CNRS, Chemin de Bellevue, BP110,
F-74941, Annecy-le-Vieux

Abstract

The predictions of the PYTHIA6.205 and PHOJET1.12 MC event generators for diffractive processes and minimum bias events are presented for the LHC energy. The comparison with the experimental data from the ISR, the SPS and the Tevatron is made.

1. Introduction

In the proton-proton interactions it is customary to distinguish between elastic and inelastic processes. Again, it is conventional to divide inelastic processes into diffractive and non-diffractive ones. Non-diffractive events are usually called *minimum bias events*. Diffractive processes include single and double diffractive dissociation and central diffraction. at the LHC energy it is expected a pure double pomeron exchange in the central diffractive production [1]. Thus, we can write the total proton-proton cross-section as the following series

$$\sigma_{tot} = \sigma_{elas} + \sigma_{inelas} = \sigma_{elas} + \sigma_{mb} + \sigma_{dif} = \sigma_{elas} + \sigma_{mb} + \sigma_{sd} + \sigma_{dd} + \sigma_{cd} \quad (1)$$

A good description of the soft hadronic interactions at the LHC energy is a necessary tool to calculate the feasibility of any experiment that must be able to separate the interesting processes from the large quantities of events produced in proton-proton interactions at high energy. The pileup of many soft interactions in the trigger gate adds a non negligible noise on top of the interesting events making more complex their analysis.

At present, different phenomenological models are used to describe the non-diffractive and diffractive processes and some of them are implemented in the Monte Carlo simulation packages (generators), like PYTHIA, PHOJET, HERWIG, ISAJET [2, 3, 4, 5]. The comparison of the different generators for minimum bias events at the LHC energy have been made in many studies (see, for example, [6]-[8]).

This report presents a study of the minimum bias and diffractive events predicted by the two Monte Carlo simulation packages PYTHIA and PHOJET compared to the available data. In what follows, PYTHIA and PHOJET should respectively be understood as PYTHIA6.205 [4] and PHOJET1.12 [5].

2. MC event generators

The PYTHIA model is described at length in [4]. Below, we point out the basic principles of the model related to the simulation of the low- p_t processes. Low- p_t processes play a dominant role in the inelastic scattering. PYTHIA uses a perturbative QCD for both low- p_t and high- p_t regions. The dominant $2 \rightarrow 2$ QCD cross-sections are divergent for $p_t \rightarrow 0$ and drop rapidly at large p_t . Probably the lowest order perturbative cross-section will be regularized at small p_t by colour coherence effects. In PYTHIA this low- p_t divergence is solved by two ways. In the first one, the so-called "simple" scenario, a cut-off parameter p_{tmin} is used, i.e. $d\sigma/dp_t = 0$ for $p_t < p_{tmin}$. In the second, the "complex" scenario, all divergent terms are corrected by a factor $p_t^4/(p_t^2 + p_{t0}^2)$ and p_t^2 in α_S is replaced by $(p_t^2 + p_{t0}^2)$. This removes the perturbative QCD divergences at low- p_t . The first is equivalent to the existence of a maximum impact parameter, b_{max} , above which there are no interactions. The second assumes that there is some matter distribution in the hadron interactions at various impact parameters. Different sets of parton distribution functions (p.d.f.) may be chosen for the proton interactions. The current version of PYTHIA uses the default p.d.f., CTEQ5L.

PHOJET is based on the Dual Parton Model¹ (see review in [16]) using another mechanism in the low- p_t region than perturbative QCD. PHOJET can be considered as a two-component model with a smooth transition between the soft and the hard regions at some p_{tmin} . PHOJET can simulate 8 basic scattering processes separately or simultaneously. They include all processes mentioned in equation (1) as well as quasi-elastic scattering and hard direct interactions. Unlike PYTHIA, the central diffraction with double pomeron exchange is included in the PHOJET tools. PHOJET, has been tuned to the minimum bias data from CDF at 1800 GeV.

HERWIG [2] is based on the UA5 results and ISAJET [3] on the Abramovskii-Kancheli-Gribov model. These simulation packages represent more simple models than PYTHIA and PHOJET without the smooth transition between the soft and hard physics. In [6] it is shown that HERWIG and ISAJET have a large divergence with the CDF data for its inclusive p_t spectrum as well as for its pseudorapidity distributions of charged particles.

3. Cross-sections

In PYTHIA, the total cross-section is calculated through the Regge theory according to the following sums of powers [17]:

$$\begin{aligned}\sigma_{tot}^{pp} &= 21.70s^{0.0808} + 56.08s^{-0.4525} \\ \sigma_{tot}^{p\bar{p}} &= 21.70s^{0.0808} + 98.39s^{-0.4525}.\end{aligned}$$

The first term in these expressions corresponds to the Pomeron exchange and the second one to the Reggeons (ρ, ω, f, a) exchanges. Because the Pomeron has the quantum numbers of the vacuum, its couplings to the proton and anti-proton are equal, so the coefficient 21.70 is the same for σ_{tot}^{pp} and $\sigma_{tot}^{p\bar{p}}$. At high energy the Reggeon term becomes negligible, $\sigma_{tot}^{p\bar{p}} \simeq \sigma_{tot}^{pp}$, so we can use for the generator comparison the experimental data from pp as well as $p\bar{p}$. In PHOJET, the cross-section is calculated according to the two component Dual Parton Model using the optical theorem [18]. The PYTHIA and PHOJET predictions for pp total cross-section are shown in fig.1. Their simulated cross-sections are compared with the existing pp and $p\bar{p}$ experimental data [19]. Both generators have a good agreement in the region below 700-800 GeV. Fig.4 shows that for higher energies the predictions are different, coming up to 18 % divergence at ~ 10 TeV. For the LHC energy ($\sqrt{s} = 14$ TeV) PYTHIA and PHOJET predict $\sigma_{tot}^{pp} = 101.5$ mb and 119 mb, respectively (see table 1). Fig. 1 shows that PHOJET is in agreement with the CDF data and in disagreement with the E710 and E811 data at the Tevatron energy.

The elastic cross-sections calculated by both generators are shown in fig. 2 and compared with the experimental data. As previously, the predictions start to diverge at energies higher than 700 GeV (the divergence is ~ 55 % at the LHC energy). The PYTHIA

¹The Dual Parton Model is a phenomenological realization of the large N_c, N_f expansion of QCD [9] in connection with the general ideas of duality [10] and the Gribov's reggeon field theory [11].

and PHOJET predictions for the elastic cross-section at the LHC energy are respectively 22.2 mb and 34.4 mb (see table 1). The difference between the total and the elastic cross-sections giving the inelastic cross-section is shown in fig. 3 for both generators and compared with the experimental data. For the inelastic cross-section, the divergence between the two predictions is not large (6.6 % at the LHC energy).

In fig. 5 the PYTHIA and PHOJET calculations are compared with the available experimental data for single (a) and double (b) diffractions. In PYTHIA, single and double diffractive cross-sections are calculated using the triple-pomeron approximation [20, 21] in the so-called Born graph approach. But the experimentally observable diffractive cross-sections are considerably smaller than the Born graph calculations.

Although data on single diffractive cross-sections have large uncertainties, the rise of the cross-section from the ISR energies to the energies of the $Spp\bar{S}$ and the Tevatron, see fig. 5a, cannot be explained at the Born level. In the PHOJET model, a special eikonal unitarization procedure is used to suppress the strong rise of the triple pomeron exchange. This is the reason of the large divergence between the PYTHIA and PHOJET predictions for the single and double diffractive cross-sections. This divergence becomes larger at higher energies and reaches 22 % for single diffraction and 58.5 % for double diffraction at the LHC energy (see table 1).

Process	PYTHIA σ^{pp} , mb	PHOJET σ^{pp} , mb	Difference, %
Elastic	22.2	34.4	54.9
Inelastic	79.3	84.5	6.6
Minimum bias	55.2	68.0	23.1
Single diffraction	14.3	11.0	22.0
Double diffraction	9.8	4.06	58.5
Central diffraction	—	1.42	—
Total cross-section	101.5	119	17.2

Table 1: Differences between the PYTHIA and PHOJET pp cross-sections at $\sqrt{s} = 14$ TeV.

Central diffractive events are simulated in PHOJET only. In this diffraction process, the double pomeron exchange dominates at high energy. The PHOJET prediction for the central diffractive cross-section is shown on fig. 5c. In both generators, the minimum bias cross-section is calculated according to series (1) by subtracting the diffractive cross-section from the inelastic one: the result is shown on fig. 5d. The minimum bias cross-sections obtained at the LHC energy are 55.2 mb with PYTHIA and 68 mb with PHOJET. Figure 4 summarizes the difference between the PYTHIA and PHOJET cross-sections at the LHC energy for all processes listed in the series (1).

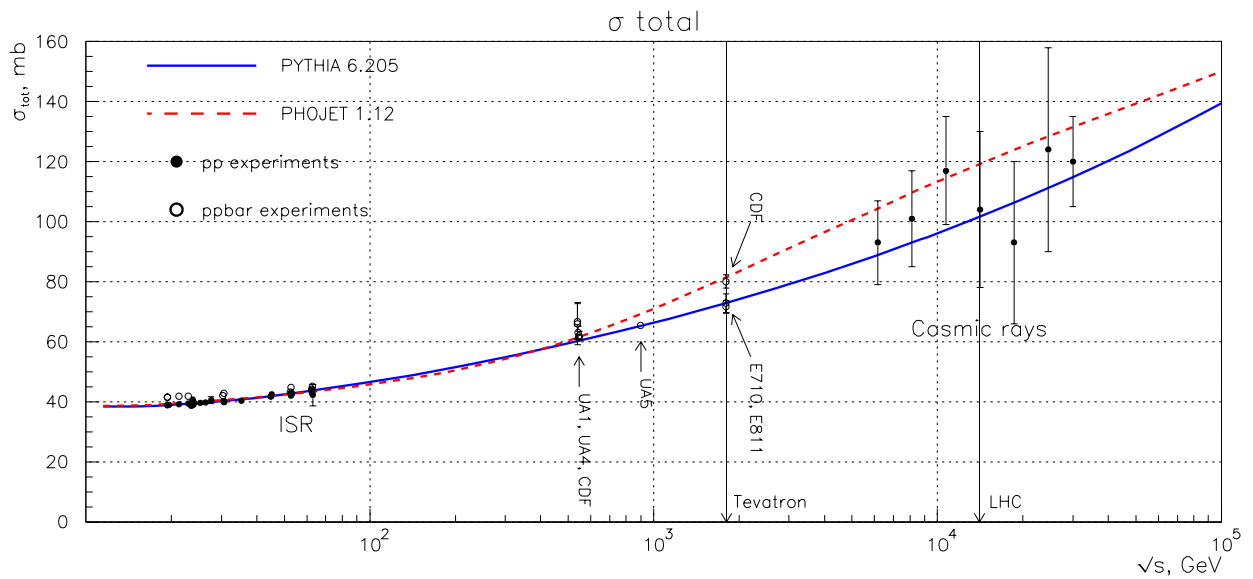


Figure 1: Predictions for the pp total cross-sections from PYTHIA (solid line) and PHOJET (dotted line). The experimental data for total cross-sections are shown for pp collisions (black circles) and for $p\bar{p}$ collisions (white circles) (data files by courtesy of the COMPAS Group, IHEP, Protvino, Russia).

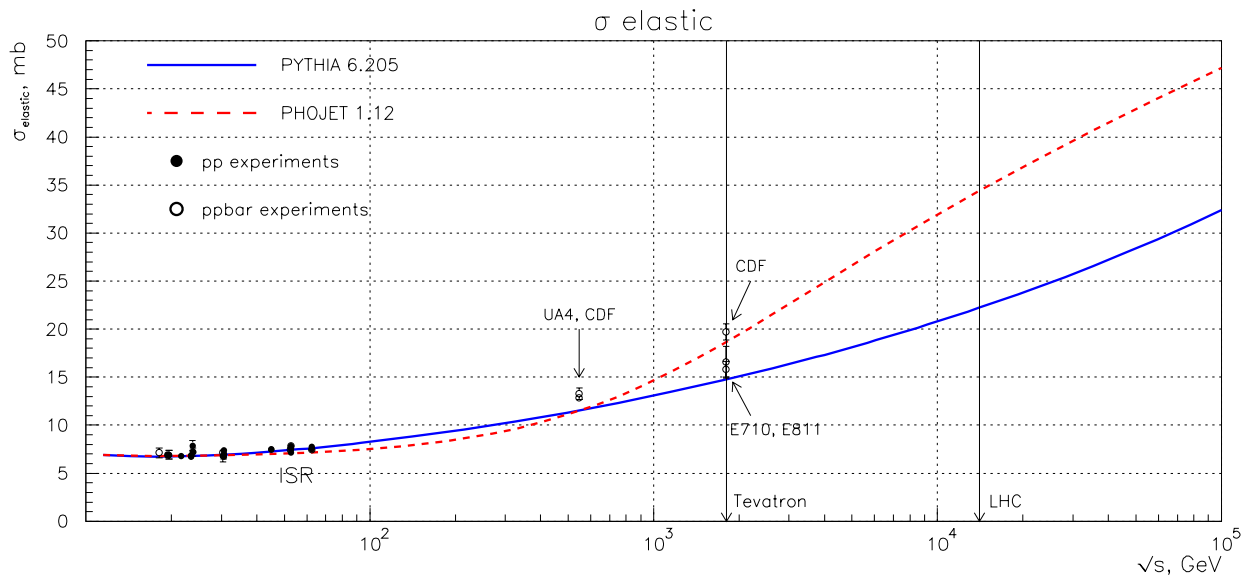


Figure 2: The same plot as in fig.1 for the elastic cross-sections.

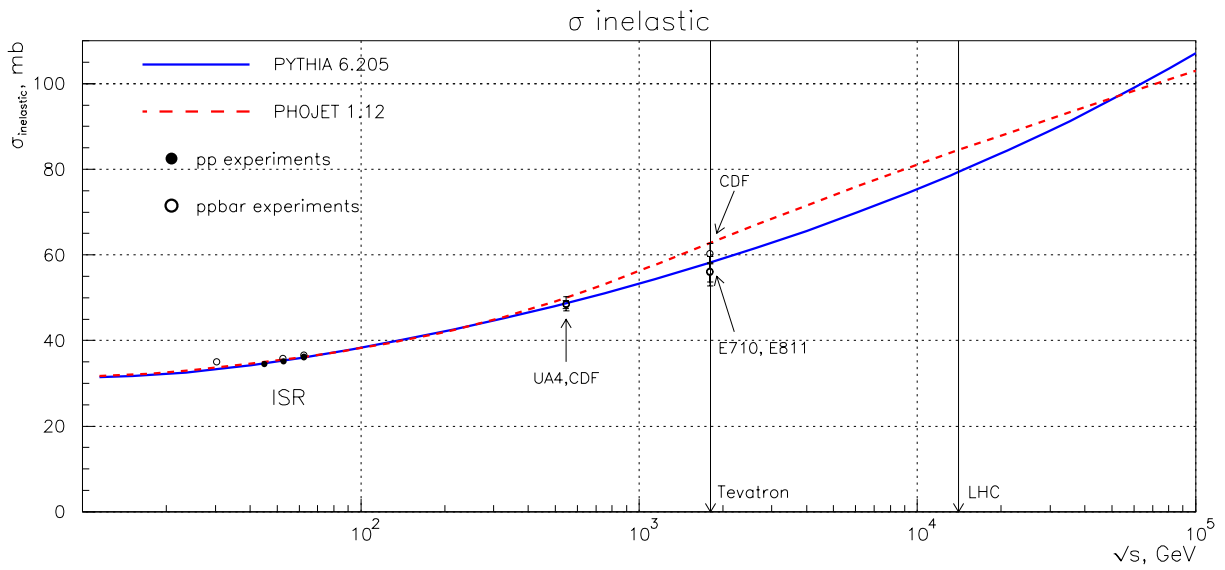


Figure 3: The same plot as in fig.1 for the inelastic cross-sections.

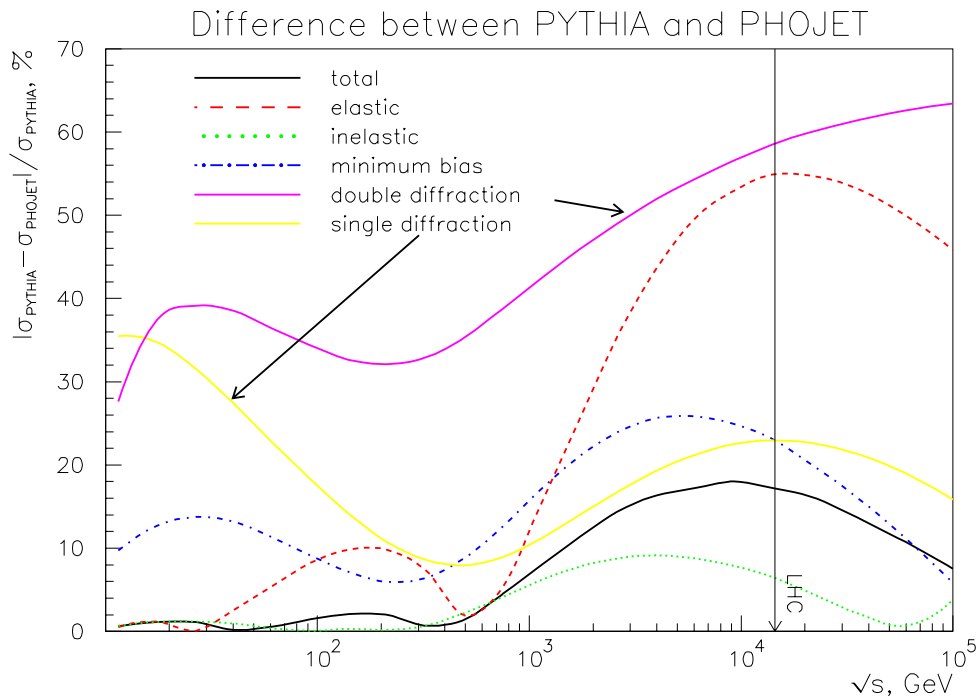


Figure 4: Difference between PYTHIA and PHOJET.

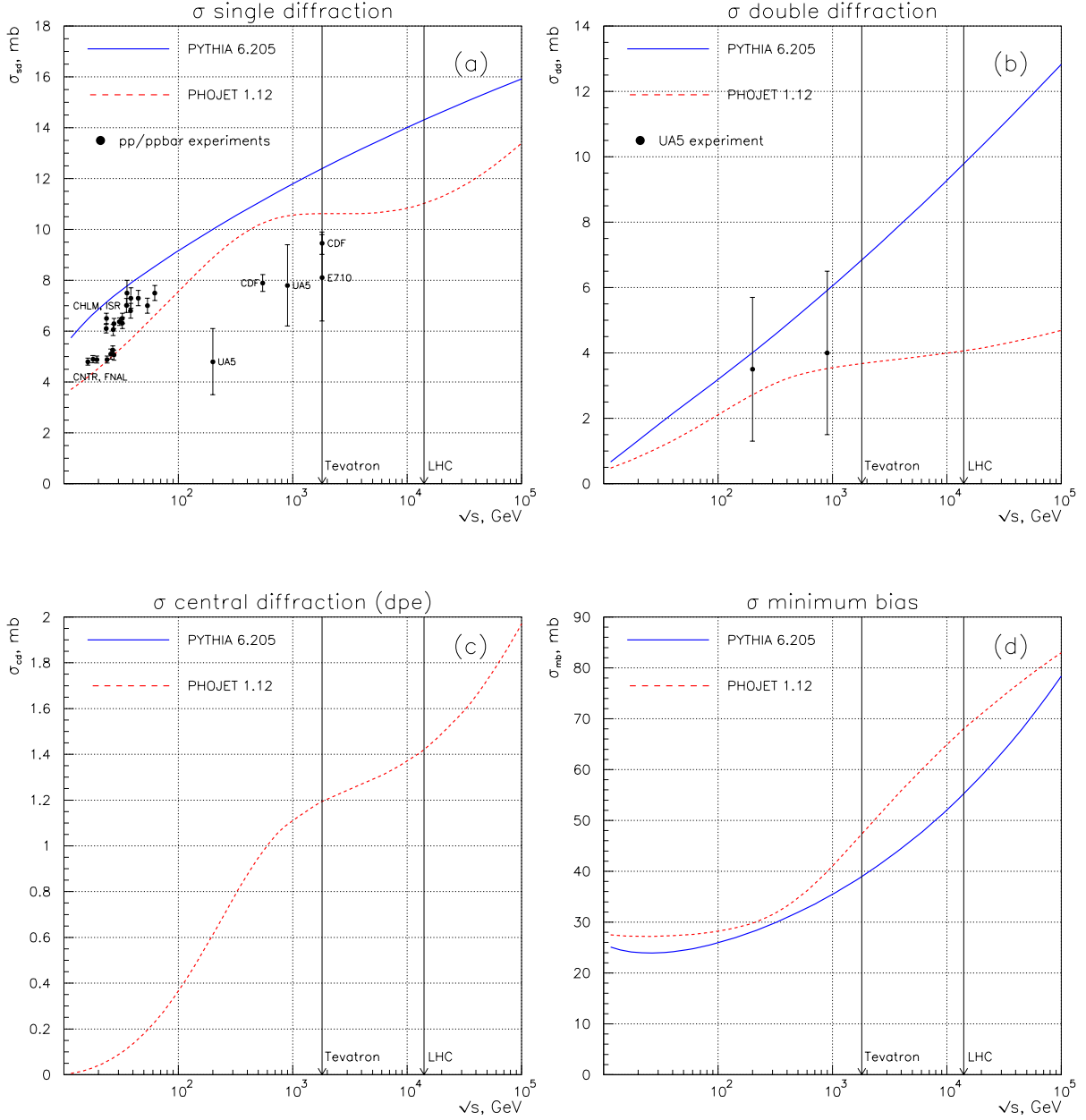


Figure 5: PYTHIA (solid line) and PHOJET (dotted line) cross-sections for a) single diffraction, b) double diffraction, c) central diffraction and d) non-diffractive production (minimum bias). The experimental data for single diffractive cross-sections [22]-[27] and double diffractive cross-sections [26] are shown on figures a) and b) respectively.

4. Minimum bias

The generation of non-diffractive processes in PYTHIA can be done in different ways, varying the solution of the divergence problem (see chapter 2), the value of the cut-off parameter, the type of the parton distribution function and so on. The different scenarios of interaction can be chosen with the value given to the keys MSTP and PARP. We studied the most commonly used scenarios (see table 2) for the non-diffractive simulations and compared them to the available data from UA5 [12] and CDF [13].

Scenario	Parameters	Explanation	p.d.f.
1, PYTHIA	MSTP(82)=1	"simple" scenario with p_{tmin} cut-off	CTEQ5L
2, PYTHIA	MSTP(82)=4	"complex" scenario (model for multi-parton interactions: varying impact parameter and a hadronic matter overlap consistent with a double gaussian matter distribution given by PARP(83) and PARP(84) (resp. default = 0.5 and 0.2) and with a continuous turn-off of the cross-section at $p_{t0}=\text{PARP}(82)$ (see scenarios 3 and 4)	CTEQ5L
3, PYTHIA	MSTP(82)=4 MSTP(2)=2 MSTP(33)=3 PARP(82)=1.9	"complex" scenario 2nd order running to α_S K factor (a K-factor is introduced by a shift in the $\alpha_S(Q^2)$ argument, $\alpha_S = \alpha_S(\text{PARP}(33)Q^2)$ in accordance with [14]) p_{t0} calculation (regularization scale of the transverse momentum spectrum for multiple interactions tail)	CTEQ5L
4, PYTHIA	MSTP(82)=4 MSTP(2)=2 MSTP(33)=3 PARP(82)=2.3	"complex" scenario 2nd order running to α_S K factor (see scenario 3) p_{t0} calculation (recommended by [15])	CTEQ5L
PHOJET	IPRON(1)=1	minimum bias	GRV94L

Table 2: Parameters for the different scenarios of low- p_t events generation.

The result of this comparison is shown in fig. 6. The charged particles density $dN_{ch}/d\eta$ has been calculated as a function of the pseudorapidity η for the scenarios listed in table 2 for non-single diffractive events (NSD) at $\sqrt{s} = 200$ and 900 GeV compared to the UA5 data and at $\sqrt{s} = 1800$ GeV compared to the CDF data. Moreover, the same distributions have been calculated for inelastic events (NSD+SD) at $\sqrt{s} = 200$ and 900 GeV compared to the UA5 data².

²There is no data for inelastic processes from CDF.

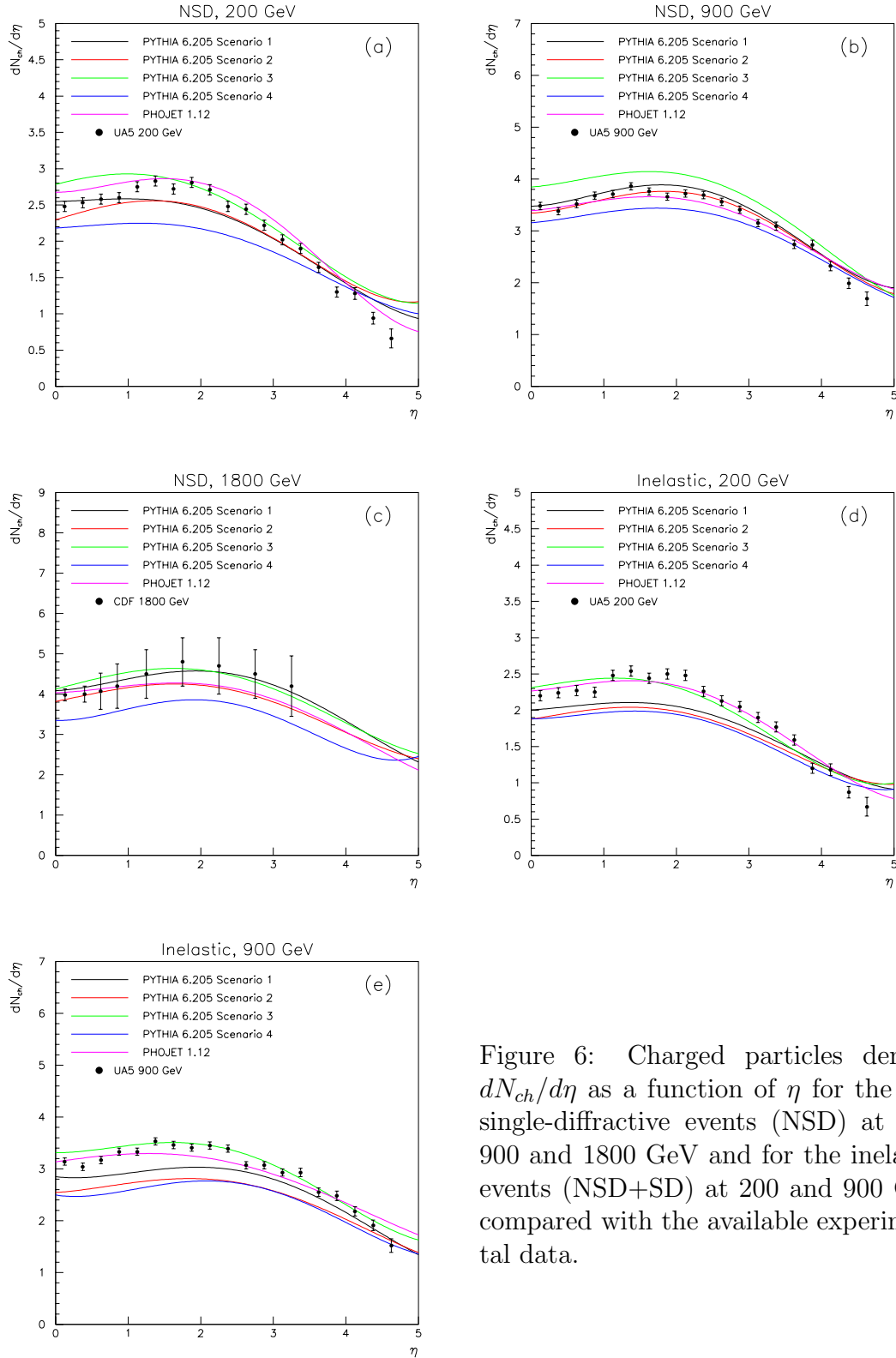


Figure 6: Charged particles density $dN_{ch}/d\eta$ as a function of η for the non single-diffractive events (NSD) at 200, 900 and 1800 GeV and for the inelastic events (NSD+SD) at 200 and 900 GeV compared with the available experimental data.

With the scenario 3 PYTHIA gives the best description of the experimental data for the inelastic events at 200 and 900 GeV and for NSD events at 200 and 1800 GeV. For this reason we will use this scenario for further calculations. PHOJET, with its default parameters, describes fairly well the inelastic as well as the NSD data at all studied energies. Thus, PYTHIA (scenario 3) and PHOJET (default set of parameters) are in a reasonable agreement with the experimental data and among themselves.

However, there is a difference between these two MC generators at higher energy and this becomes more and more evident with the rise of the energy. The left part of fig.7 shows the central rapidity density of the charged particles $dN_{ch}/d\eta(\eta = 0)$ plotted as a function of the c.m. energy. The PYTHIA and PHOJET predictions are compared to the NSD data from UA5 and CDF. The dotted line shows the fit to the experimental data [13]:

$$dN_{ch}/d\eta(\eta = 0) = 0.023\ln^2(s) - 0.25\ln(s) + 2.5.$$

At the LHC energy this fit to the experimental data gives $dN_{ch}/d\eta(\eta = 0) = 6.2$, when PYTHIA and PHOJET respectively predict 7.1 and 4.8 charged particles at $\eta = 0$ for the NSD events. Thus allowing to consider PYTHIA and PHOJET as high and low extreme limits for the charged particles multiplicity at energies higher than 1 TeV.

The right part of fig. 7 shows the estimations of PYTHIA and PHOJET for the

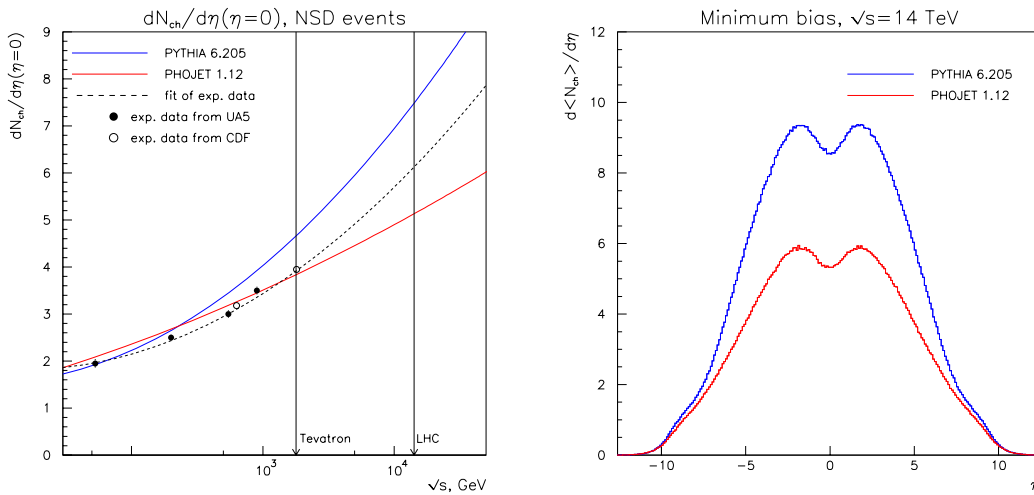


Figure 7: On the left: central rapidity charged particles density $dN_{ch}/d\eta(\eta = 0)$ plotted as a function of the c.m. energy. The PYTHIA and PHOJET predictions are compared to the NSD data from the UA5 and CDF experiments. On the right: PYTHIA and PHOJET predictions for the density $dN_{ch}/d\eta$ of charged particles produced in non-diffractive processes at the LHC energy.

density of charged particles $dN_{ch}/d\eta$ produced in non-diffractive processes at the LHC energy. The charged particles densities, predicted by PYTHIA and PHOJET in the central pseudorapidity region are respectively 8.5 and 5.3. Table 3 shows the predictions of PYTHIA and PHOJET for the average particle multiplicity for a proton-proton minimum bias event at the LHC energy.

Minimum bias, $\sqrt{s} = 14$ TeV		
Particles	PYTHIA	PHOJET
p	4.56	3.15
\bar{p}	3.38	1.97
n	7.24	4.66
$\pi^+\pi^-$	88.5	57.3
γ	103.6	4.9
K^+K^-	10.08	7.13
K_L	4.89	3.54
$\mu^+\mu^-$	0.023	0.018
e^+e^-	1.19	0.075
<i>Neutrinos</i>	0.018	0.017
$N_{charged}$	107.8	70.61
N_{total}	223.6	121.5

Table 3: Average particle multiplicity for a proton-proton minimum bias event obtained by PYTHIA and PHOJET at the LHC energy.

5. Diffractive processes

5.1 Single diffraction

In order to compare the PYTHIA and PHOJET predictions for single diffractive production we used the $p\bar{p}$ experimental data of the UA4 Collaboration [28]. UA4 measured the pseudorapidity distributions of charged hadron production for different masses of the diffractive system. We have compared these data with PYTHIA and PHOJET (see fig. 8). We have also compared the mean charged particle multiplicity in the diffractive hadronic system measured for several masses by UA4 with the predictions of PYTHIA and PHOJET (see fig. 9). It is evident from fig. 8 and 9 that PHOJET, taking in account the contributions from the hard diffractions (minijets) and the multiple soft interactions, has a better description of the data than PYTHIA, taking in account the Born term contributions only.

Moreover, we have calculated with PYTHIA and PHOJET some typical distributions characterizing the single diffractive production: the pseudorapidity and the p_t distribu-

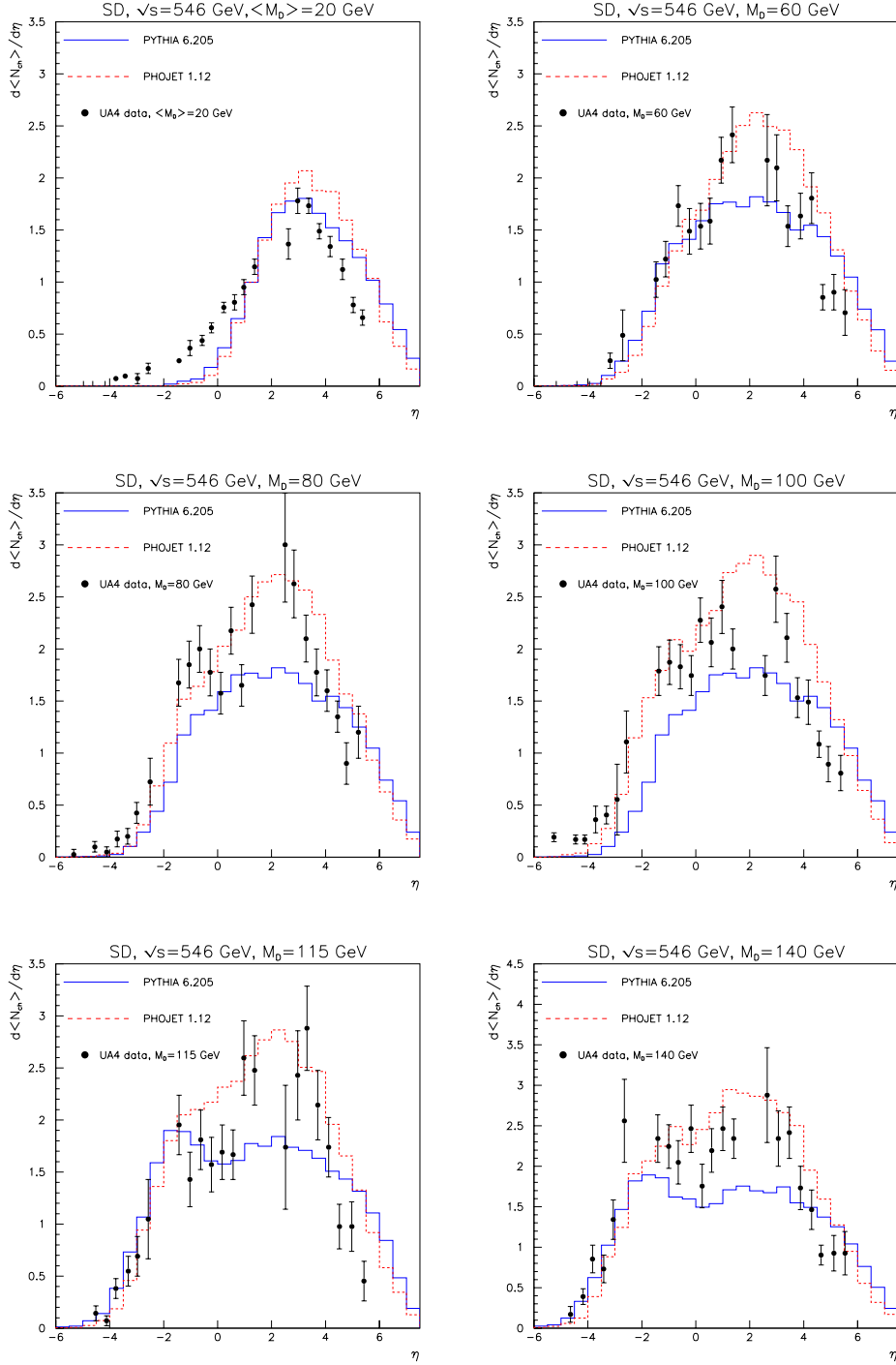


Figure 8: Pseudorapidity distributions of the charged hadrons in SD compared to the UA4 data for different masses of the diffractive system.

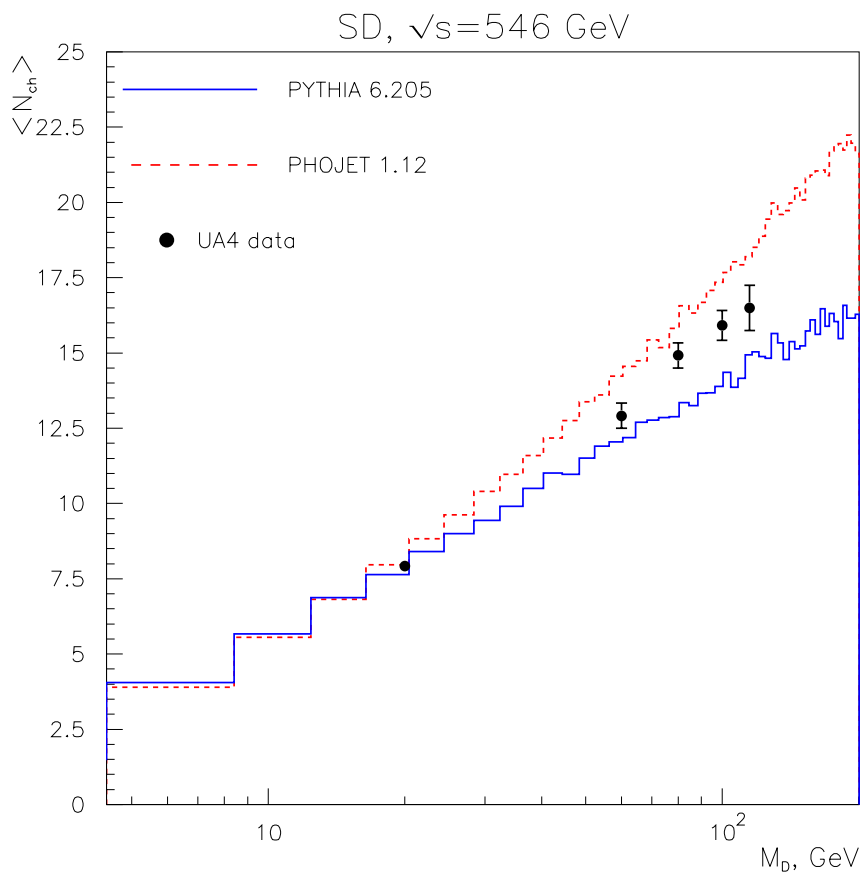


Figure 9: Average charged particle multiplicity produced in SD as a function of the invariant mass of the diffractive system compared to the UA4 data.

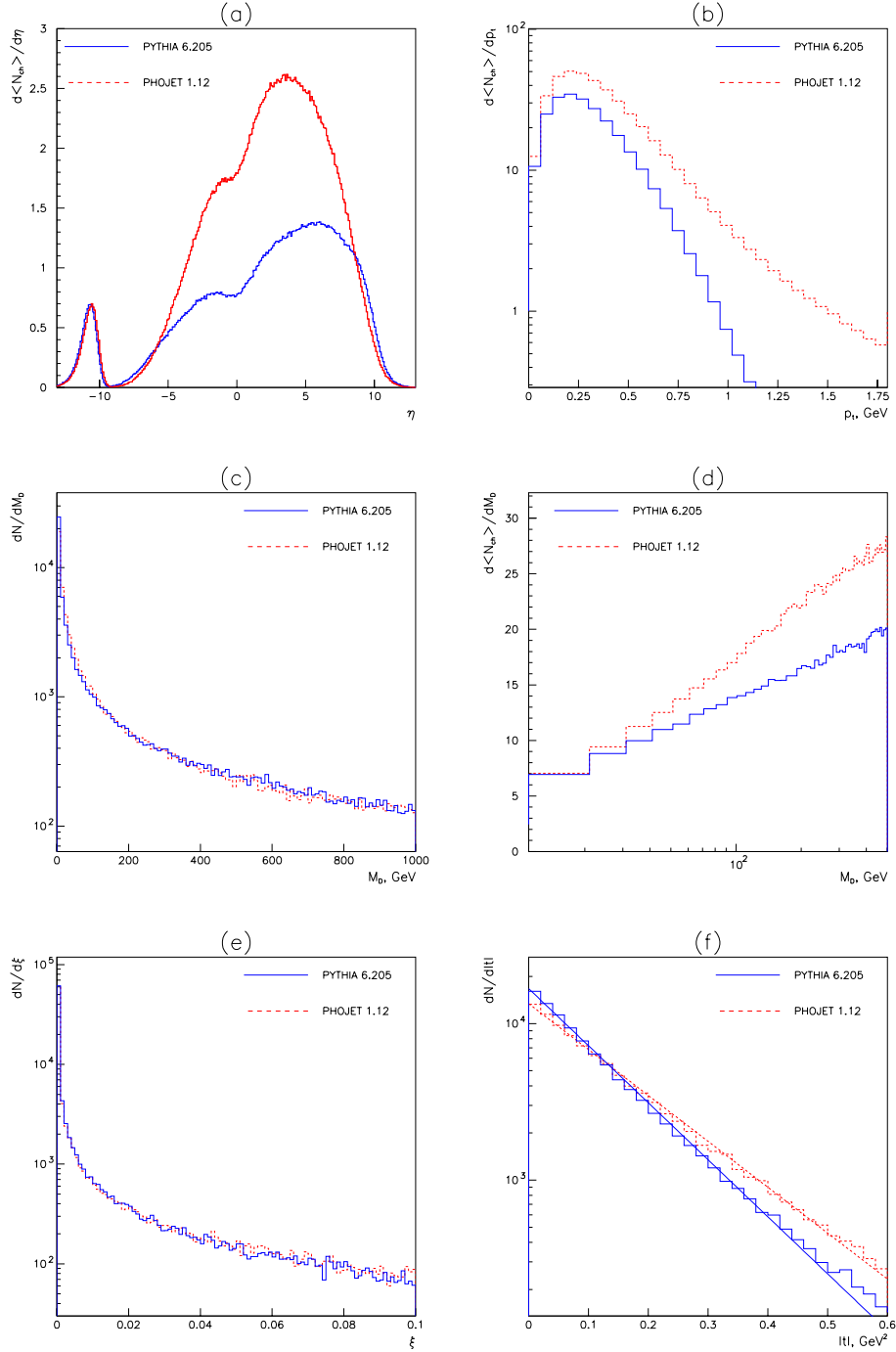


Figure 10: PYTHIA and PHOJET predictions for SD at the LHC energy: (a) charged particles pseudorapidity distribution; (b) charged particles p_t distribution; (c) mass of the diffractive system; (d) average charged particle multiplicity as a function of the diffractive system mass; (e) ξ and (f) t distributions of the scattered proton (see text).

tions of the charged particles in the diffractive system, the distribution of the diffractive mass, the dependence of the average charged particle number in the diffractive system on the mass of the diffractive system, at last, the $\xi = \delta p/p$ (the relative momentum loss) and the t (the transverse momentum squared) distribution of the scattered proton (see fig. 10).

In PYTHIA as well as in PHOJET the differential cross-sections, $d^2\sigma/dtdM^2$, are exponential in t and $\sim 1/M^2$:

$$\frac{d^2\sigma}{dtdM^2} \sim \frac{1}{M^2} e^{-bt}, \quad (2)$$

where M is the mass of the diffractive system and t is the transverse momentum squared of the scattered proton. t , ξ and ϕ , the azimuthal angle, define the kinematics of the scattered proton. In a single diffractive scattering $pp \rightarrow pX$:

$$M^2 = s\xi. \quad (3)$$

PYTHIA and PHOJET have a small difference in the t distribution (fig. 10f). The slope parameter b is equal to 8.39 in PYTHIA and to 6.75 in PHOJET.

As above mentioned, there are large divergences between PYTHIA and PHOJET in the predictions of the charged particle multiplicity in the diffractive system, this is shown in fig. 10 (a), (b) and (d). Table 4 and fig. 10 (a) show that PHOJET predicts a multiplicity 1.6 times larger than PYTHIA.

Single Diffraction, $\sqrt{s} = 14$ TeV		
Particles	PYTHIA	PHOJET
p	2.05	2.32
\bar{p}	0.48	0.71
n	1.34	1.71
$\pi^+\pi^-$	13.01	22.35
γ	15.30	1.85
K^+K^-	1.34	2.75
K_L	0.65	1.33
$\mu^+\mu^-$	0.0006	0.007
e^+e^-	0.18	0.03
<i>Neutrinos</i>	0.0004	0.006
$N_{charged}$	17.06	28.47
N_{total}	34.35	48.14

Table 4: Average particle multiplicity in the diffractive system produced in SD obtained by PYTHIA and PHOJET at the LHC energy.

5.2 Double diffraction

Some distributions characterizing a double diffractive production have been obtained by PYTHIA and PHOJET (see fig. 11). These are the pseudorapidity and the p_t distributions of charged particles in the diffractive system, the distribution of the diffractive mass, the dependence of the mean charged particles number in the diffractive system on the mass of the diffractive system.

As in the case of single diffraction a large divergence in the charged particles multiplicity between PYTHIA and PHOJET is observed (see table 5), the predictions of the charged particles multiplicity differ by a factor 1.7.

Double Diffraction, $\sqrt{s} = 14$ TeV		
Particles	PYTHIA	PHOJET
p	1.70	2.07
\bar{p}	0.55	0.86
n	1.90	2.32
$\pi^+\pi^-$	16.55	29.15
γ	19.54	2.38
K^+K^-	1.63	3.47
K_L	0.78	1.69
$\mu^+\mu^-$	0.001	0.008
e^+e^-	0.24	0.033
<i>Neutrinos</i>	0.0006	0.006
$N_{charged}$	20.67	35.96
N_{total}	42.88	61.62

Table 5: Average particle multiplicity in the diffractive system produced in DD obtained by PYTHIA and PHOJET at the LHC energy.

5.3 Central diffraction

Finally, we present some characteristic distributions for the central diffractive production at the LHC energy (see fig. 12). They have been generated by PHOJET with its default parameters as PYTHIA has no possibility to simulate central diffractive production.

The differential cross-section is described by equation (2), but the relation (3) should be changed to

$$M^2 = s\xi_1\xi_2, \quad (4)$$

where ξ_1 and ξ_2 correspond to the 2 scattered protons in the central diffraction $pp \rightarrow pXp$.

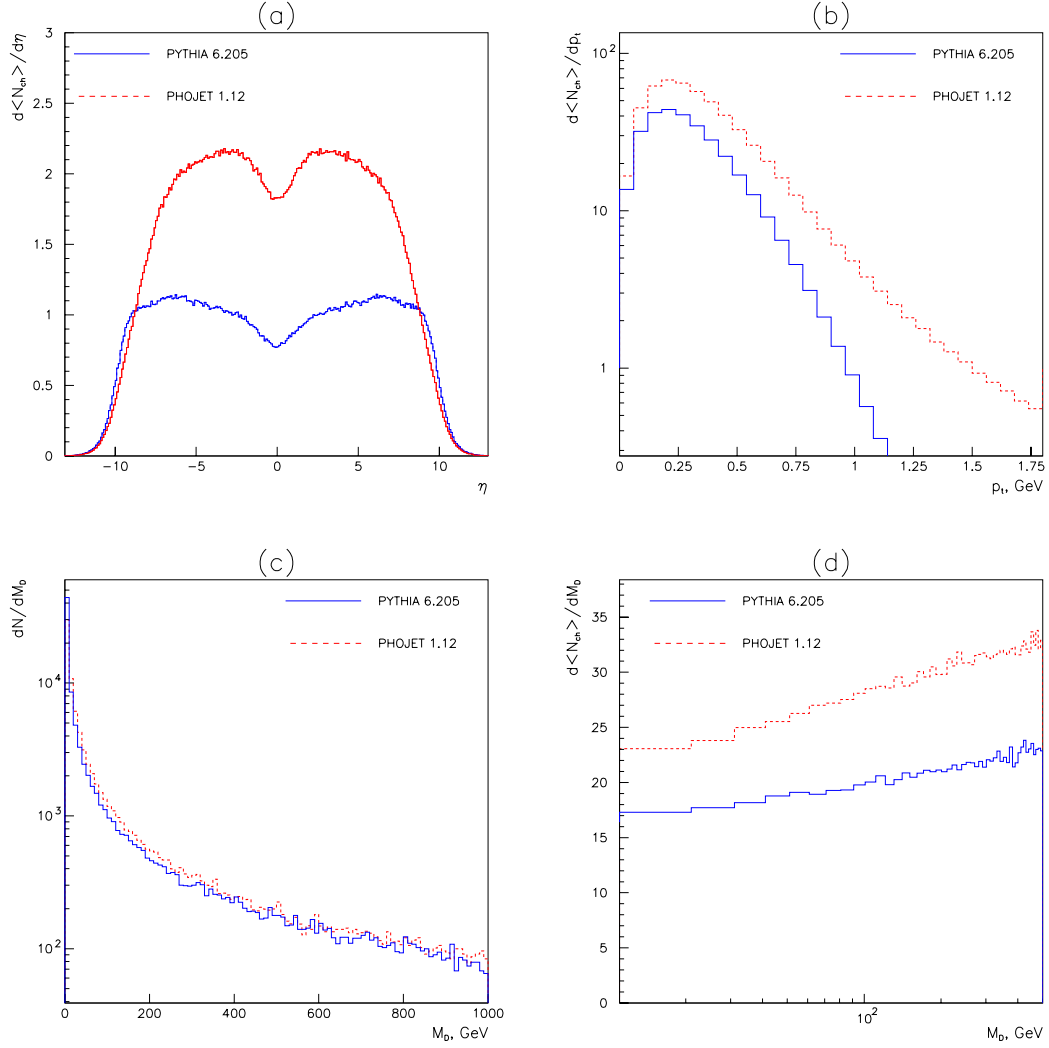


Figure 11: PYTHIA and PHOJET predictions for DD at the LHC energy: (a) charged particles pseudorapidity distribution; (b) charged particles p_t distribution; (c) mass of the diffractive system; (d) average charged particle multiplicity as a function of the diffractive system mass.

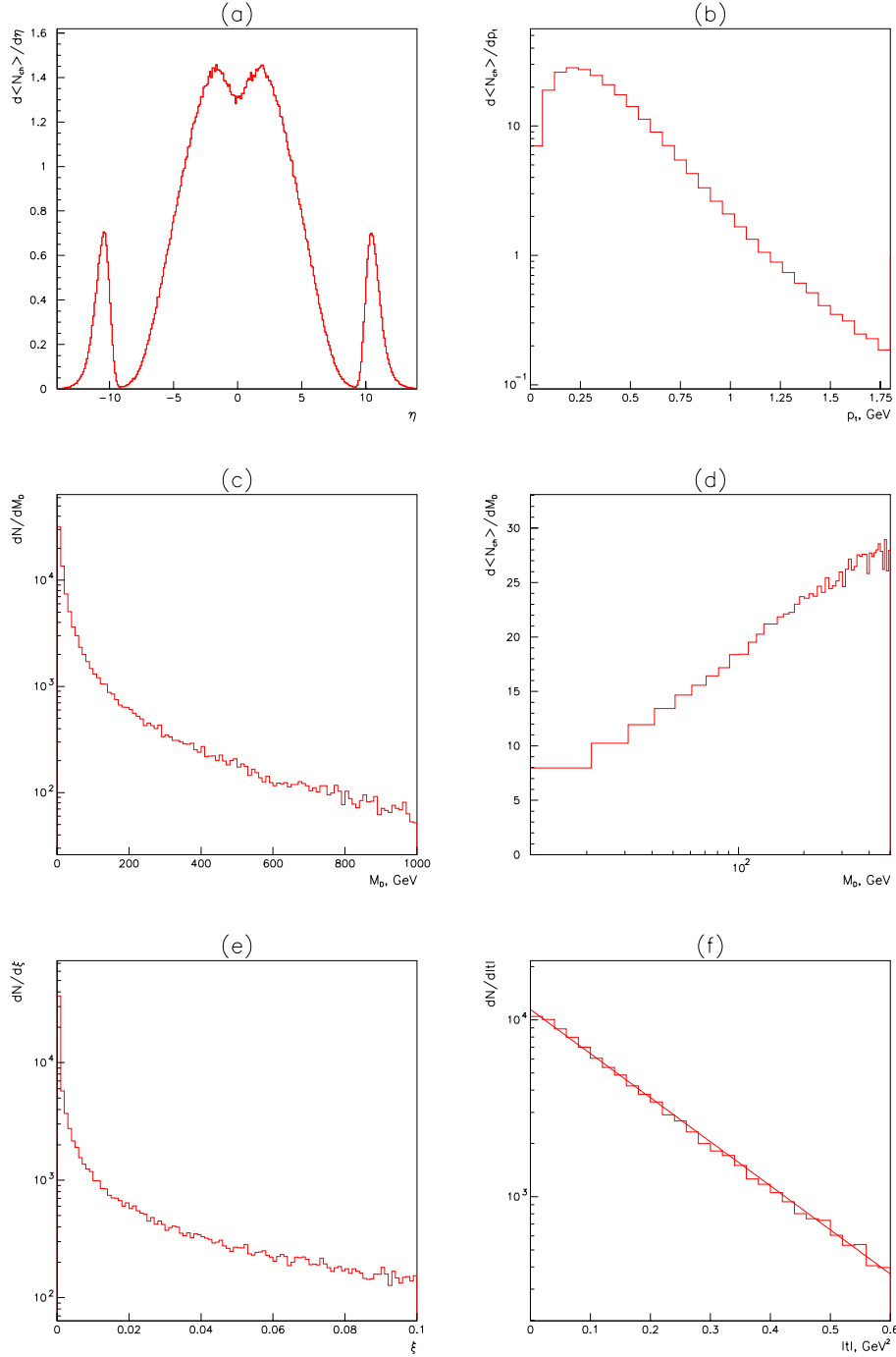


Figure 12: PHOJET predictions for CD at the LHC energy: (a) charged particles pseudorapidity distribution; (b) charged particles p_t distribution; (c) mass of the diffractive system; (d) average charged particle multiplicity as a function of the diffractive system mass; (e) ξ and (f) t distributions of the scattered protons.

The distributions of the central diffractive mass, ξ and t of the scattered protons are respectively shown in fig. 12 (c), (e) and (f). The slope parameter b of the t -dependence is 5.73.

The density of the charged particles as a function of the pseudorapidity is shown in fig. 12a in which the left and right peaks in the region $|\eta| > 9$ are due to the scattered protons. The charged particles from the central diffractive system are distributed in the region $|\eta| < 9$. Around $\sim 30\%$ of the charged particles from the central diffractive system fall into the TOTEM [29] acceptance ($3 < |\eta| < 7$). Around 60% of the charged particles lie in the acceptance of the CMS tracker covering the η region from -3 to 3.

Central Diffraction, $\sqrt{s} = 14$ TeV	
Particles	PHOJET
p	2.36
\bar{p}	0.36
n	0.72
$\pi^+\pi^-$	12.31
γ	1.02
K^+K^-	1.53
K_L	0.75
$\mu^+\mu^-$	0.003
e^+e^-	0.01
<i>Neutrinos</i>	0.003
$N_{charged}$	16.73
N_{total}	27.29

Table 6: Average particle multiplicity in the diffractive system produced in CD obtained by PHOJET at the LHC energy.

As it was mentioned in the introduction, it is expected a pure double pomeron exchange in the central pp collisions and no contamination of any reggeon exchanges at the LHC energy. It makes this reaction to be a pure source of gluon rich states and glueballs. It is necessary to note that, in addition to glueballs, the study of the double pomeron exchange at the LHC energy gives the unique opportunity to make exclusive measurements of the Higgs production using the CMS+TOTEM facility [30].

6. Conclusion

We have compared the predictions of the PYTHIA and PHOJET MC event generators with the available experimental data from the ISR, the SPS and the Tevatron. Also we have compared the predictions of PYTHIA and PHOJET for minimum bias events and diffractive processes at the LHC energy.

There are large divergences between PYTHIA and PHOJET in the prediction of the cross-sections. They start to differ at energies $600\div 700$ GeV. The difference in elastic and double diffractive cross-sections becomes larger than 50 % at the LHC energy, while the difference in single diffractive and non-diffractive cross-sections remains at the level of $22\div 23$ %. The reason of such a large discrepancy lies in the different models used by PYTHIA and PHOJET for the cross-section calculations. Unlike PYTHIA, PHOJET suppresses the diffractive cross-sections at high energy providing a reasonable description of the existing experimental data.

On the basis of the comparison of the PYTHIA predictions for the charged particle density in non-single diffractive and inelastic events to the UA5 and CDF data, we would recommend to use the set of parameters called Scenario 3 (see table 2) for any minimum bias simulation. This scenario of PYTHIA or PHOJET, with its default parameters, give a reasonable description of the experimental data at different energies up to 1800 GeV. However, these two generators differ at higher energy and the differences in the predictions become larger with the rise of the c.m. energy.

The comparison of the PYTHIA and PHOJET simulations to the UA4 data for single diffraction shows that PHOJET describes the diffraction processes better than PYTHIA. We have also compared PYTHIA and PHOJET for single and double diffraction at the LHC energy. PHOJET predicts ~ 2 times larger charged particles multiplicities.

Acknowledgments

The authors are grateful to M.Bozzo, K.Eggert, F.Ferro and M.Macri for helpful discussions. We also thank E. and G. Sobol for their help for the numeralization of some plots with the experimental data.

References

- [1] S.N.Ganguli and D.P.Roy Phys.Rep. **67** (1980) 203.
- [2] G.Marchesini *et al.*, Comp. Phys. Commun. **67** (1992) 465.
- [3] F.E.Paige, S.D.Protopopescu, *ISAJET manual*.
- [4] T.Sjöstrand Computer Physics Commun. **82** (1994) 74.
- [5] R.Engel *PHOJET manual, V1.05c*, June 1996. Available from: [http : //www – ik.fzk.de/ engel/phojet.html](http://www-ik.fzk.de/engel/phojet.html).
- [6] A.Kupčo, ATL-PHYS-99-019, November 1999.
- [7] A.Moraes, I.Dawson and C.Buttar, ATL-PHYS-2003-020, July 2003.

- [8] G.Ciapetti and A. di Giaccio, Proceedings of the LHC workshop, vol.2, CERN 90-10, p.155.
- [9] G.Veneziano, Nucl. Phys. **B74** (1974) 365.
- [10] G.F.Chew and C.Rosenzweig, Phys.Rep. **41** (1978) 263.
- [11] V.N.Gribov and A.A.Migdal, Sov.J.Nucl.Phys. **8** (1969) 583.
- [12] G.J.Alner *et al.*, Z. Phys. **C33** (1986) 1.
- [13] F.Abe *et al.*, Phys. Rev. **D41(7)** (1990) 2330.
- [14] R.K.Ellis and J.C.Sexton, Nucl.Phys. **B269** (1986) 445.
- [15] <http://amoraes.home.cern.ch/amoraes/underlying/underlying.html>
- [16] A.Capella *et al.*, Phys. Rep. **236** (1994) 227.
- [17] A.Donnachie and P.V.Landshoff, Phys.Lett. **B296** (1992) 227.
- [18] R.Engel, Z.Phys.**C** 66 (1995) 203.
- [19] K. Hagiwara *et al.*, Phys. Rev. **D66** (2002). Data files from <http://wwwppds.ihep.su:8001/hadron.html>, by courtesy of the COMPAS Group, IHEP, Protvino, Russia.
- [20] G.A.Schuler and T.Sjöstrand, Phys.Lett., **B407** (1993) 539.
- [21] G.A.Schuler and T.Sjöstrand, Phys.Lett., **B376** (1996) 193.
- [22] CNTR Collab., J.Schamberger *et al.*, Phys. Rev. Lett. **34** (1975) 1121.
- [23] CHLM Collab., M.G.Albrow *et al.*, Nucl. Phys. **B108** (1976) 1.
- [24] CHLM Collab., J.C.M.Armitage *et al.*, Nucl. Phys. **B194** (1982) 365.
- [25] CDF Collab., F.Abe *et al.*, Phys. Rev. **D50** (1994) 5535.
- [26] UA5 Collab., R.E.Ansorge *et al.*, Z. Phys. **C33** (1986) 175.
- [27] E710 Collab., N.A.Amos *et al.*, Phys. Lett. **B301** (1993) 313.
- [28] U4 Collab., D.Bernard *et al.*, Phys. Lett. **B166** (1986) 459.
- [29] V. Berardi *et al.* CERN-LHCC-2004-002, Jan 2004.
- [30] J.P.Guillaud and A.Sobol, LAPP-EXP-2003-009.